sciendo

POLISH MARITIME RESEARCH 3 (115) 2022 Vol. 29; pp. 176-186
10.2478/pomr-2022-0038

A METHOD FOR THE INTERPRETATION OF SONAR DATA RECORDED DURING AUTONOMOUS UNDERWATER VEHICLE MISSIONS

Mariusz Zieja [1, *]
Wojciech Wawrzyński [2]
Justyna Tomaszewska [3]
Norbert Sigiel [4]

[1] Air Force of Technology, Warsaw, Poland
[2] Warsaw University of Technology, Poland
[3] Military University of Aviation, Dęblin, Poland
[4] MCM Squadron, Gdansk, Poland

* Corresponding author: *mariusz.zieja@itwl.pl (M. Zieja)*

ABSTRACT

Image acquisition from autonomous underwater vehicles (AUVs) is useful for mapping objects on the seabed. However, there are few studies on the interpretation of data collected with side-scan sonar during autonomous underwater vehicle missions. By recording the seabed with 3D multibeam sonar, a large number of survey points can be obtained. The collected data are processed using applications based on remote sensing image processing. The data collected during AUV missions (or other sonar carriers) needs to be pre-processed to reach the proper effectiveness level. This process includes corrections of signal amplification (Time Varying Gain, or TVG) and geometric distortions of sonar images (Slant Range Corrections). It should be mentioned that, when carrying out the interpretation process for structures on the sea floor, sonar users need to understand the process of visualising seabed projections and depressions, as well as the resolution limitations of the sonar sensors.

Keywords: onar technologies; sea floor monitoring; autonomous underwater systems.

INTRODUCTION

During both world wars, tens of thousands of sea mines were laid in the Baltic Sea, a significant number of which still remain on the seabed and pose a significant threat to shipping and the marine environment. According to the Baltic Marine Environment Protection Commission 'HELCOM', during World War II alone, some 40,000 tonnes of chemical ammunition was also dumped into Baltic waters.

The environment will deteriorate because of the length of time the objects have been on the seabed, the associated progressive corrosion and poor water exchange in the Baltic Sea. The location of these objects, and their protection or destruction, is a significant challenge for the countries around the Baltic Sea. Due to rapidly developing autonomous systems, there are new possibilities for detecting, classifying and identifying the threat. For this reason, the exploration of marine waters is extremely necessary since, in many areas (particularly those difficult to access by humans), the level of the threat is still unknown. Therefore, in order to expand the explored areas, data are collected from sensors mounted on underwater vehicles. Image acquisition from underwater vehicles is useful for mapping objects on the seabed [1]. The data collected in this way make it possible to identify objects on the seabed, such as sunken ships. Having accurate maps of the seabed is important to ensure safe transport. Therefore, more and more attention is being paid to the development of rapid methods for object detection and the monitoring of possible obstacles in maritime transport routes [2]increasing attention is being paid to the development of effective methods for the

detection and monitoring of possible obstacles on the transport route. Bathymetric laser scanners record the full waveform reflected from the object (target. Modern developments in obtaining spatially correct digital data from side-scan sonar systems have resulted in images that can, subsequently, be processed, enhanced, and quantified. With appropriate processing, these acoustic images can be made to resemble easily recognisable optical photographs.

The first operators of Synthetic Aperture Sonar (SAS) were military users. In particular, they are used in large areas where small, low-signature bottom mines need to be detected and classified in a short amount of time and with sufficiently high resolution [3]. The technology also has a number of other potential applications, including seabed exploration, underwater archaeology, mapping debris, and search and rescue operations.

Vehicles used for seabed exploration can be divided into two main groups: manned and unmanned operating vehicles. Within unmanned underwater vehicles (UUV), two groups can be distinguished: Remotely Operated Vehicles (ROV) and Autonomous Underwater Vehicles (AUV). AUVs can be classified as: underwater glider, underwater propeller AUV and biomimetic AUV [4]. The main differences between the different types of UUVs, such as ROV and AUV, lie in their mode of operation. The first is remotely controlled and the second is highly automated and carries out tasks independently. In some cases, only second-class vehicles are regarded as autonomous robots.

Each of these platforms has various imaging and mapping capabilities, appropriate for specific scales and tasks [5]. They gain the necessary information through on-board sensors and systems. Every AUV, in its most basic form, must have a navigation system, a propulsion system and a dry, watertight environment for placing on-board components. In addition, an AUV is typically equipped with systems and components such as a diving system, microcontroller, attitude control, power supply and sonar [6]. By providing a synthetic aperture, the sonar is able to overcome physical limitations and achieve higher resolution, compared to side-scan sonar (SSS), which is a different technique for obtaining underwater images. In order for the sonar to work properly, the UUV must move less than one-half the physical length of the antenna between pings (a pulse of sound created by active sonar). By moving slightly less, overlapping data can be used to estimate the platform's movement with an incredible degree of accuracy. The maximum reachable coverage using SAS is, therefore, inversely proportional to the platform speed. This means that the area coverage rate is dependent of speed and directly coupled to the length of the receiver array. Acoustic cameras (sonars) are the most suitable sensors because they provide acoustic images with more precision than other sensors, even in turbid water [7]. The most popular configuration of sonar sensors used to monitor underwater obstacles is a forward-looking sonar (FLS) [8]with one of the most popular configurations being forward looking sonar (FLS. A Gaussian Particle Filter (GPF), based on the tracking approach, is used to more accurately identify objects to solve the problem of persistently tracking multiple targets in a noisy environment. It is based on the nature of acoustic-visual images and modified signal filtering, as well as growing regional segmentation methods to improve image processing performance. Secondly, a generalised regression neural network is adopted to evaluate multiple features of target regions and the representation of feature subsets is developed to improve tracking performance [9]. Recently, one of the methods used for underwater image reconstruction is analysing data from 3D optical sensors. Together with distributed scalable big data, storage and artificial intelligence in automated 3D metrology is a powerful tool in the investigation of the seabed 10].

Although sonar data displayed on a screen can be interpreted by inexperienced operators, the effectiveness of the whole operation can be significantly increased when users of the sonar systems have a basic knowledge. Effective sonar record interpretation requires taking into account many factors, including complex processes of data collection and environmental restrictions, as well as platform characteristics. The article includes recommendations and guidance for operators, which are helpful during sonar record interpretation, and mainly focuses on the data obtained during autonomous underwater vehicle (AUV) missions. Previous works related to the subject mostly cover the aspects of side scan sonar data received using towed sonars [11, 12]. However, the basic principles of sonar operation are the same. There are some differences concerning the sonar records acquired during AUV missions, which will be described in this paper. The first section covers the characteristics of side scan sonar geometry. The second section describes characteristic sonar record disruptions and AUV mission planning aspects. The last sections are dedicated to the proper interpretation of objects and sea bottom structures. This work includes examples of sonar records of real objects.

RELATED WORKS

Researchers have acknowledged a growing interest in the interpretation of AUV imagery in various disciplines, e.g. maritime archaeology, geology and military applications. One of the last explored methods is automatic target recognition for small autonomous vehicles with the usage of efficient deep learning algorithms. As Topple and Fawcett [13] pointed out, advances in deep learning have managed object detection using data from a variety of sensor types. This was achieved by adapting neural network-based models trained on large datasets from natural images, which are commonly applied to the remote sensing (RS) domain through transfer learning. Unfortunately, the limitations of small hardware, such as computational performance and battery power, reduce the possibility of running deep learning models on board. Standard pre-trained object detection models include large conventional neural networks requiring tens to hundreds of billions of floating-point operations to distinguish multiple object classes in natural images. Indeed, such large models may be too complex for the tasks performed by sonar. Consequently, [13]

proposed the MiNet system, which was successfully deployed aboard the Ocean Server Iver small AUV during the REBOOT sea trials and predicted the width, length and class of objects detected in sonar images within minutes of the completion of each mission stage.

In another method described by Yu et al. [14]the first step in side-scan sonar (SSS, side-scan radar data was used (the method consisting of four main steps) to visualise the data. Firstly, the raw SSS data were analysed to obtain a greyscale image and the blind zone boundary of the image was obtained using a threshold method. Secondly, the noise characteristics of the image were analysed and the de-noising algorithm optimised to effectively remove high-frequency noise. Then, spatial-temporal matching calculations were performed for each port and starboard ping and the accurate coordinates of the first bottom returns were obtained by extreme value detection. Finally, automatic and accurate bottom line detection was performed according to the smooth processing of the coordinate sequence of the first bottom returns.

In Zhang et al. [15]the point target reference spectrum (PTRS, the authors described multi-receiver synthetic aperture sonar and proposed a new method for providing high-resolution images in systems. In the proposed method, the point target reference spectrum (PTRS), azimuth modulation, and coupling term were deduced based on an accurate time delay. This modification of the PTRS method has an advantage over the traditional one, in which algorithms are still exploited.

The image generation method presented by Chen et al. [16] was based on a retinex algorithm using a two-sided filtering process, colour pre-correction, estimated reflectivity and dynamic range. Compensation, colour compensation and other processes realise the accurate perception of underwater targets using an extended Kalman filter (EKF) and spatial feedback linear transformation matrix. The target range method was used to solve the joint angles of the manipulators and target tracking and grasping were then completed. Underwater experiments showed that the algorithm not only improved the dynamic stability of AUVs but also ensured the grasping accuracy of the underwater robot and optimised the control performance of the system.

Considering that de-noising and detection of underwater sonar images are crucial for proper image interpretation, Wang et al. [17] proposed a new adaptive approach to address this issue. Firstly, an adaptive method for de-noising non-local spatial information based on the golden ratio was proposed and, secondly, a new adaptive cultural algorithm (NACA) was offered to precisely and quickly complete the process of detection. The next step was the development of image generation and interpretation, as an alternative for the fuzzy clustering method and Markov segmentation algorithm. Although their results were satisfactory, the processing procedures are quite complex and computationally costly.

Last but not least, the advanced Automatic Target Recognition (ATR) method applied by Isaacs [18], for unexploded ordnance (UXO) detection and classification using sonar data from open ocean survey sites, should be mentioned. The classic paradigm of anomaly detection in images breaks down in cluttered and noisy environments. After an upgrade, and when more robust object detection is performed using an in-situ weighted highlight-shadow detector, features are generated on geometric moments in the imaging domain and, finally, classification is performed using an Ada-boosted decision tree classifier. This method is widely used for military purposes.

Sonar data processing is also one of the daily responsibilities of the research centre at the NATO Centre for Maritime Research and Experimentation, which is working on the utilisation of robotics in minefields, to deliver doctrinally relevant autonomy and on-board intelligence. Research on improving the quality of image signals is being conducted by the Naval Undersea Warfare Center, Maritime Technologie und Forschung, the Centre for Maritime Research and Experimentation and the Atlantic Research Centre, among others.

SIDE SCAN SONAR GEOMETRY

Sonar signals are broadly classified as either passive or active. The sound waves generated by sea creatures, the motors of ships, or the sea itself (i.e. waves) are passive sonar signals, whereas radar signals are active sonar signals. With active signals, a sonar device (a sonar transducer) produces sounds and then analyses the echo. In this research, the data from SSS has been used. SSS is easily accessible and economic to use to get images of the seabed and underwater objects. Object and target detection based on SSS images has a wide diversity of applications for military purposes; it is increasingly used for the identification and categorisation of mines.

The images discussed in the following section were generated using an algorithm for AUV route generation, which was designed to reduce the time needed to prepare a mission plan, taking into account the environmental and vehicle-specific characteristics. This algorithm can be summarised in the following way:

- The starting point for the development of the programme was the data acquired during the research, concerning both the architecture of a given subsystem, its tactical data (manoeuvring elements, energy consumption, accuracy of geographic positioning during mission execution, etc.), as well as the characteristics of the operating environment (in this case, the Baltic Sea area).
- The main parameters entered in the algorithm were: geographical position of the area of operations, AUV Altitude, AUV Speed, Course, Water Depth, speed of sound propagation in water (SVP) and a theoretical range of the sonar.
- After entering the parameter values, the operator can generate a mission plan using three modes: planning based on sonar near/far ranges, planning based on AUV speed, or planning based on object detection probability.
- The process is then optimised. The optimal distribution of the search pattern and the optimal trajectory of the AUV should provide full area coverage. For the systems

equipped with side-looking sonars, the lawnmower pattern gives a possibility to cover the nadir gap below the sonar transducer. The distance between the mission plan line is determined by the sonar detection ranges, i.e. the maximum and the minimum. For the vehicle equipped with synthetic aperture sonar where the detection ranges depend mainly on vehicle speed, the minimum and maximum values can be determined experimentally for the specified AUV speed. The optimal trajectory of the autonomous vehicle can be determined by implementing the transformations from the projection of the geographic coordinates describing the area of operation into a mission plan, in a format acceptable by the manufacturer's software.

The key to the proper interpretation of collected data is knowledge concerning side scan sonar geometry and sonar carrier characteristics (Fig. 1). In the classic configuration, the sonar carrier moves along a known trajectory and through an antenna, which main azimuth leaf is perpendicular to the direction of the carrier's motion radiates the observed area with an acoustic wave [19]. The echo signals reflected from the object are returned to the antenna, where they are received, processed and presented on the screen of the operator's console. The delay time between the signal generation and reception determines the longitudinal resolution of presented images.

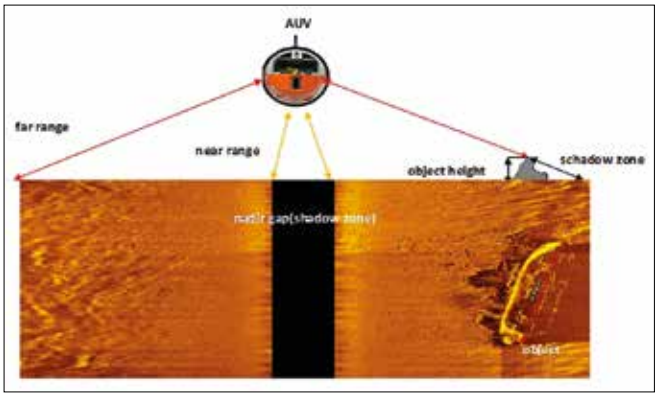

Fig. 1. Side-scan sonar geometry.

Assuming range gates of duration τ, the two seafloor objects O1 and O2 are separated by ΔR_g and will be resolved if their returns do not overlap in time (Fig. 2). The round-trip travel time for a pulse associated with the object at range R_s is given by [20]:

$$t = \frac{2R_s}{c}, \tag{1}$$

The incremental delay due to the proximate object O2 is:

$$t + \tau = \frac{2(R_s + \Delta R_s)}{c}, \tag{2}$$

where:

c – is the propagation speed in the medium (e.g. seawater),

τ – is the delay interval between the transmission and the reception of the pulse,

R_s – is the instantaneous slant range measured from the sensor to a point on the seafloor,

ΔR_s – is the range of the separation of the two seafloor objects O1 and O2.

A measure of the slant plane separability is obtained by subtracting Eq.(1) from Eq.(2), and is given by:

$$\tau = \frac{2\Delta R_s}{c}, \tag{3}$$

The relationship between ground–plane and slant-plane (Fig. 2 (left)) is approximated as:

$$\Delta R_g = \frac{\Delta R_s}{cos\theta_g}, \tag{4}$$

where: θ_g is the grazing angle.

Therefore, two objects on the seafloor are fully resolvable if their ground separation satisfies:

$$\Delta R_g \geq \frac{c\tau}{2cos\theta_g}, \tag{5}$$

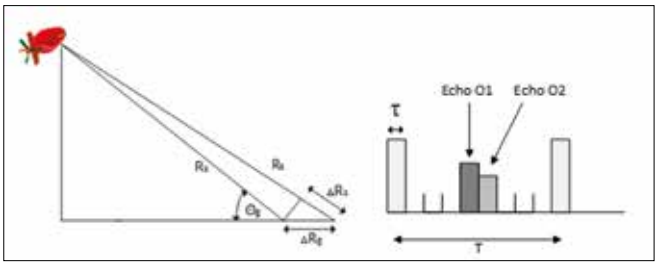

Fig. 2. Time domain representation of transmitted pulse and corresponding echoes [20] (Licensee IntechOpen).

Fig. 3 shows the slant-plane view of side-looking sonar with a projector of length D and azimuth beam width Θ_H. The parameters δ_a^{min} and δ_a^{max} correspond to the linear azimuth beam width at the minimum and maximum slant ranges, respectively. The half-power angular beam width of a uniformly weighted rectangular aperture of length D is given in by the approximate relationship [20]:

$$\Theta_H = \frac{\lambda}{D}, \tag{6}$$

where λ is the acoustic wavelength of the signal.

The resolution of a side looking sonar system at slant range distance R_s is given by:

$$\delta_a \cong \frac{R_s\lambda}{D}. \tag{7}$$

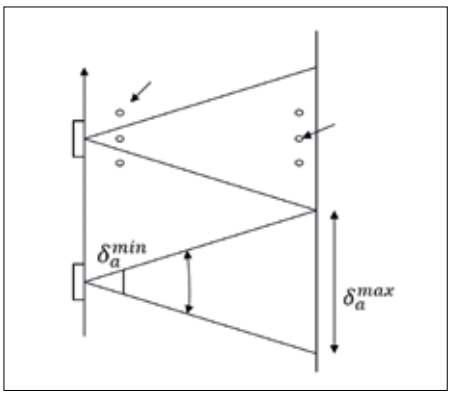

Fig. 3. Slant range, along-track SAS geometry with a beam spread as a function of slant-range [20] (Licensee IntechOpen).

In order to keep the resolution small as the range increases,

the frequency and/or the physical aperture length D must be increased. The azimuth resolution, however, will depend on the slant range [20].

Conventional sonar usually uses the same transducers to generate the signal and to receive the echo from an object. One of the examples of that solution is the GAVIA autonomous underwater vehicle, equipped with the conventional side looking sonar EDGETECH. New solutions have recently appeared, which separate the transmitter and receiver array, e.g. AUV HUGIN equipped with HiSAS sonar. In both cases, sonar image creation is connected with precise counting of the time between the signal generated by the transmitter and the echo received from the object in the water column or on the seabed. Nowadays, the systems equipped with synthetic aperture sonar technology provide possibilities to generate higher resolution images, which means higher quality of data, with the same pulse frequency (Fig. 4) [21].

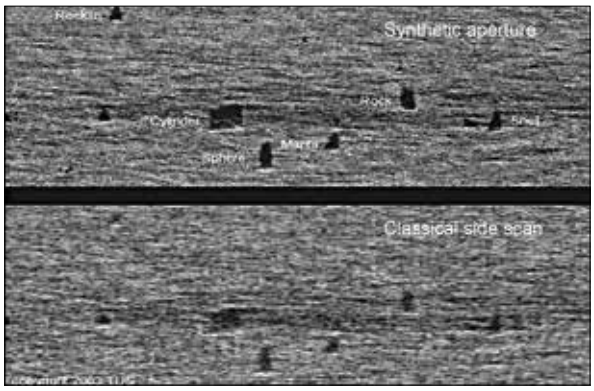

Fig. 4. Comparison of synthetic and classical side scan apertures for the equal sonar frequency [21] (copyright TUS).

FACTORS AFFECTING THE QUALITY OF SONAR DATA

The remote sensing modalities available for underwater purposes (acoustic methods) cover frequency ranges from a few Hz to a few MHz, and are the most widely used by far. Effective interpretation of the data results from a deep analysis of sonar images. The data collected during AUV missions, or other sonar carriers, need to be pre-processed to reach a proper effectiveness level [22]Polish Academy of Sciences Branch Lublin. All rights reserved. The paper includes a probabilistic method for evaluating the durability of components and device assemblies which operate under the impact of destructive processes. As a result of these processes, wear that causes deterioration of their cooperation conditions occurs. It is assumed that a component operates reliably when the wear does not exceed the acceptable (limit. This process includes corrections of the signal amplification (such as Time Varying Gain (TVG)) and geometric distortions of the sonar image (Slant Range Corrections (SRC)) [23, 24]. After SRC, the sonar images are geometrically corrected across-track; the along-track corrections account for the variations in platform speed. This process, called anamorphosis, produces an image in which the inter-pixel spacing is the same across-track and along-track [25].

Sound speed profile distribution in the water column is another source of geometric distortion, which is strictly connected with such factors as water temperature, pressure and salinity, and needs to be taken into account. These processes are the initial steps in data post-processing, which are conducted automatically without the operator's attention. Further corrections usually depend on the user's knowledge and experience and are enabled by dedicated programs for sonar record analysis, e.g. SeeTrack or Reflection. The operator can reach proper image enhancement by setting special filters, e.g. mean filter, median filter, or a palette of colours. These parameters can be selected and optimised by operators; however, there are many factors on which they have very limited influence. Characteristic distortions of sonar images result from acoustic pulse interaction with the water surface and these are presented in the following sections.

SIGNAL RETURNS FROM THE SEA SURFACE

The signal returns from the sea surface could be present in a sonar record when the sonar is closer to the surface than to the seabed. In that case, the acoustic pulse reflection from the surface will be faster than the echo from the bottom. Reflections from the surface will be present on the sonar image as an additional line. When the water surface is calm, only a thin line can be recognised. The distance between this line and the sonar is equal to the actual depth of an AUV or other sonar carrier. When the operation is conducted in different conditions, e.g. a rough sea, there is a high possibility of more extensive noise from waves, sometimes making interpretation of the data impossible. A characteristic distortion of a sonar image may also be generated by a ship's propellers. Taking safety into account during operations focusing on seabed research, there should not be any other units in the vicinity of the AUV during the mission. However, the distortion presented in Fig. 5 might appear as a result of the 'mother' ship unit being too close to the vehicle equipped with sonar. In most cases, the reason for shortening the distance between the AUV and the 'mother' ship is to improve the acoustic link capabilities. The operator should take that fact into account and keep a safe distance from the vehicle, greater than the sonar's farthest range. The distortion is visible as a white streak covering the proper data and can be generated by propellers, but also by buoys and other objects anchored in very strong currents.

Fig. 5. Distortion of sonar record caused by a ship's propellers

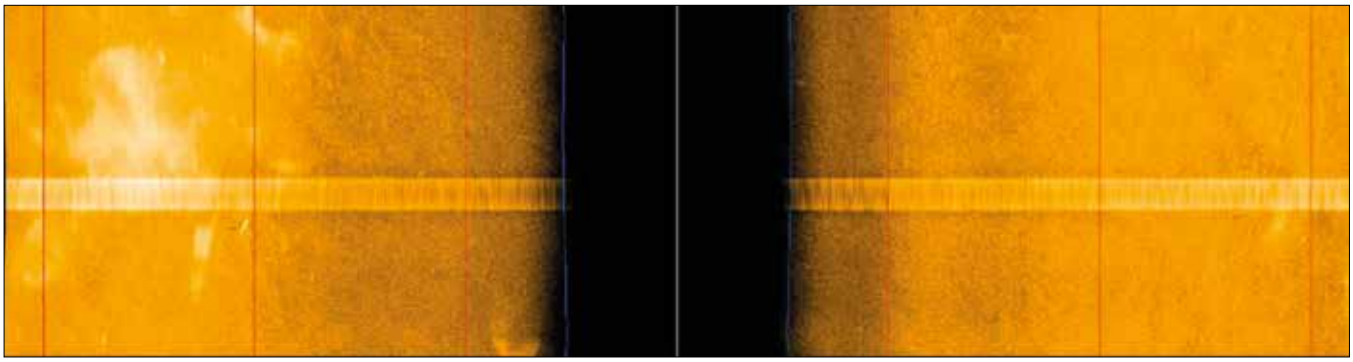

Fig. 6. Deformation of sonar image caused by environmental disruptions.

Multiple echoes from one object are another example of image disturbance. This situation is not very common and only takes place when special conditions are met, which include calm sea surfaces, shallow water areas and the presence of an object generating a very strong echo. Multiple echoes result from the different paths used by acoustic pulses to reach the object and return to the receiver. In normal conditions, the signals are moving along the way 'sonar-object-sonar'. When operating on a calm sea and shallow water, there is a possibility that additional echoes could be generated. This effect is a result of acoustic signal reflections from the surface. In that case, the signals are moving along the route: 'sonar-object-water-surface-sonar'.

Air bubbles appearing as an output of working propellers, leaking gases, and other environmental disruptions, might be another cause of obtaining improper data. When the intensity of these phenomena is very high, there is a possibility that all information from the assigned area could be lost (Fig. 6).

There may be additional restrictions relating to the specific hydrology of the area in which the operation is being conducted. One of these restrictions is connected with the sound speed profile distribution over the water column, which impacts the maximum and minimum sonar detection ranges. Fig. 7 shows that, despite the theoretical far range of sonar being equal to 180 m, useful data can only really be obtained up to 90 m from the transceiver. The other information presented on the screen does not allow operators to detect the objects of interest.

Degradation of the sonar range could appear in the area where the salty seawater is mixing with the freshwater from the rivers. The sound speed profile has a great impact on establishing sonar range. The main factor influencing the sound speed profile is temperature: a one-degree increase in water temperature results in increasing the speed of sound by 3.5 m/s. Increasing the salinity by 1 PSU causes an increase in the sound speed by 1.3 m/s, while pressure changing with the depth will increase the sound speed by 1.8 m/s for every 100 m [26]. The sound velocity value can be determined by Eq. (8) [27]:

$$C = 1449{,}2 + 4{,}6T - 0{,}55T^2 + 0{,}00029T^2 + (1{,}34 - 0{,}01T)(S - 35) + 0{,}016Z \quad \textbf{(8)}$$

where:

C – speed of sound in water, expressed in metres per second;
T – water temperature, expressed in degrees Celsius;
S – salinity, in parts per thousand;
Z – depths, in metres measured from the sea surface.

Most AUV operations require collecting and displaying data with 100% coverage of the area of interest. Full area coverage is crucial; for example, during mine countermeasure missions, confidence that all of the unexploded ordnance (UXO) has been found is an essential part of the whole mission. Taking that fact into account, the operator needs to adjust the mission plan to current environmental conditions and sonar capabilities, mainly with respect to near and far ranges. One of the most effective search patterns for an AUV vehicle equipped with side scan sonar is the 'lawnmower' pattern (Fig. 8).

The optimal distances between the mission plan lines can be determined by the equations:

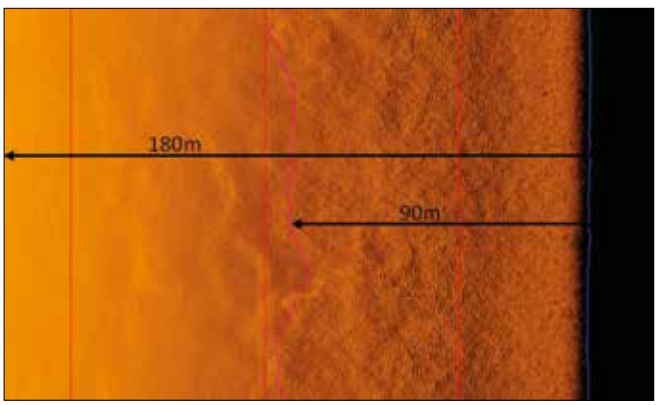

Fig. 7. Restrictions in the range of useful sonar data.

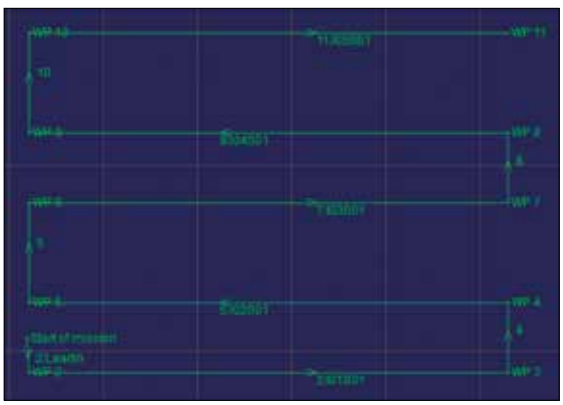

Fig. 8. AUV mission plan - lawnmower pattern tracks distribution.

$$D_{long} = 2 * R_{max} - SDNE_{AUV} - Overlap, \quad (9)$$

$$D_{short} = R_{max} - R_{min} - SDNE_{AUV} - Overlap, \quad (10)$$

where:

D_{long} – long spacing between the mission plan lines;
D_{short} – short spacing between the mission plan lines;
R_{min} – near sonar range;
R_{max} – far sonar range;
$Overlap$ – parameter used to increase the confidence that full area coverage will be achieved during the mission;
$SDNE_{AUV}$ – standard deviation of AUV navigational error.

For example, for the range values measured during this research and assuming a standard vehicle height above the bottom (i.e. 30 m), the determined values are presented in Table 1.

Tab. 1. Results of the calculation of the distance between the search strips of an AUV HUGIN vehicle.

Velocity [m/s]	The short spacing between the mission plan lines D_{short} [m].	The long spacing between the mission plan lines D [m].
1.5	138	350
2.0	83	240
2.5	58	174

The technique of distributing bands in such a way that each two neighbouring bands cover their own nadir zones makes it possible to achieve complete coverage of the area while ensuring high efficiency in the operations. The optimal selection of distances between individual lanes, taking into account the area of operation and vehicle and sonar parameters, is a complicated task which requires the consideration of many factors. Mistakes made at the planning stage may not only lead to the acquisition of poor quality data but also threaten the safety of equipment and people. In view of the above, it is important to automate the planning process and support operators, in order to ensure safety and efficiency of conducted operations.

RESTRICTIONS CONNECTED WITH SCREEN RESOLUTION AND SONAR DATA MOSAICKING PROCESS

Taking into account the efficiency of data analysis, especially during a mission focused on detecting and classifying small objects, the selection of proper monitor size and resolution, on which the data will be post-processed, is a crucial decision. Incorrect screen resolution and size could result in omitting objects, especially when the analysis is carried out over a long period of time by only one operator. Fig. 9 shows the same object presented on three different size screens and at different resolutions. During operations focusing on searching for objects which have a well-known size, knowledge about current monitor settings helps to assess the real size of the detected structure and makes it possible to carry out proper classification.

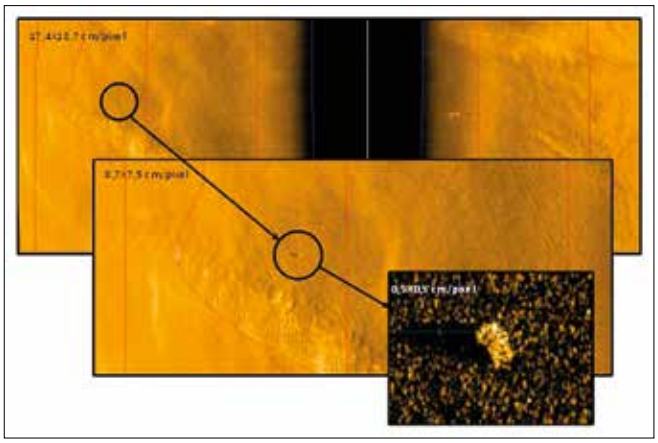

Fig. 9. Presentation of the same object at three different resolutions.

With the dynamic development of computers and informatics intended for the post-processing of hydrographic data, a new era in the field of digital sonar image (mosaic) generation has arrived. Nowadays, this process takes less time and is simplified, giving the user many devices to minimise and remove errors from the generated data. Despite the great improvements in data quality, the process of generating high-resolution mosaics is still burdened with many errors, which are the result of imperfections in sonar devices [28]. Fig. 10 presents the sonar image mosaicking errors caused by movement of the AUV during data collection.

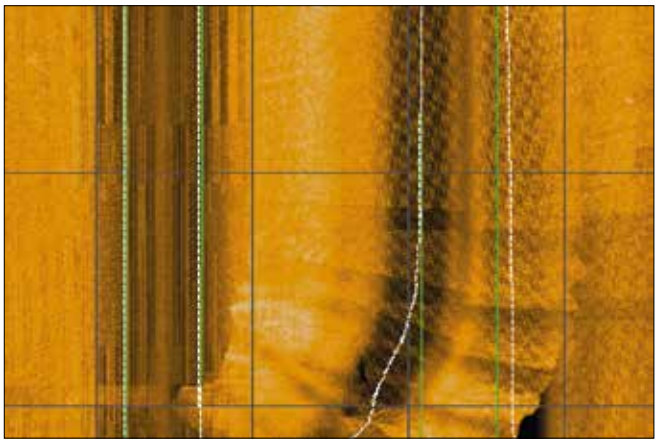

Fig. 10. Sonar image mosaicking errors caused by movement of the AUV during data collection.

VISUALISATION OF OBJECTS AND THEIR CHARACTERISTIC FEATURES

An object term is assigned to all structures recorded on the sonar screen, excluding the seabed and water surface. Objects can be located anywhere in the water space, starting from the bottom and ending at the water surface. The key factor that

helps to classify an object as a specific structure is its shadow and its presentation on the screen. During the AUV mission planning process, the operators need to focus on a few factors, which can have a great impact on further presentation of the objects. An AUV altitude affects the length of a sonar shadow and the projection of shadow on the sonar image. Shadow measurements give the operators additional possibilities for improving the classification process. These measurements are based on a simple calculation of shadow length and other dimensions of the echo (Fig. 11, Eq. (11)).

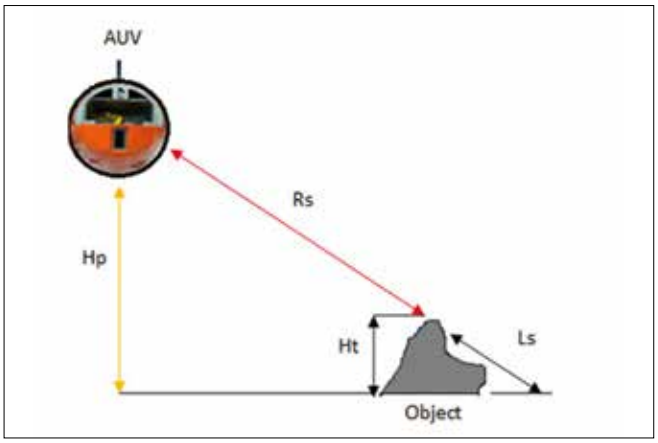

Fig. 11. Calculation concerning the height of an object based on its acoustic shadow.

$$H_t = \frac{H_p \cdot L_s}{R_s + L_s} \tag{11}$$

where:

H_t – is the height of the object;
L_s – is the length of the acoustic shadow;
H_p – is the altitude of the vehicle;
R_s – is the straight-line distance between the vehicle and the object (Slant Range) [29].

The acoustic shadow usually allows a larger amount of data to be obtained, compared to the direct reflections from an object. Fig. 12 shows that, even without the presence of a submarine kiosk on the screen, the shadow allows the operator to detect it and to measure its size.

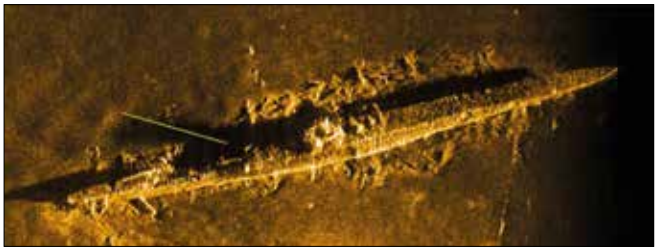

Fig. 12. Acoustic shadow providing the possibility to assess the size of the submarine vessel's kiosk.

Manmade objects usually have clearly outlined edges, while natural objects are more rounded. It is highly recommended that attention be paid to the fact that some objects may generate a very strong echo but still do not have an acoustic shadow (Fig. 13). The presence of a shadow makes it possible to assess whether the echo which has been found is true or has only appeared as a result of multipath phenomena.

Fig. 13. Object which does not have an acoustic shadow but generates a very strong echo.

The acoustic shadow provides a possibility to verify the location of an object in the water column, which clarifies if the structure is lying at the bottom or is suspended somewhere higher in the water column. Fig. 14 shows an acoustic shadow which is separated from an object by a few metres.

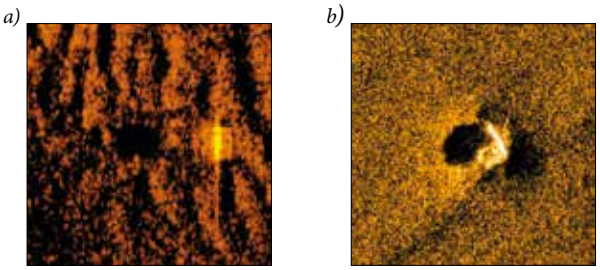

Fig. 14. Presentation of two objects, which are located: a) in the water column b) at the bottom.

When an object is located in the water column, but at a higher altitude than the autonomous vehicle, then there it is highly likely that its shadow will be invisible (Fig. 15).

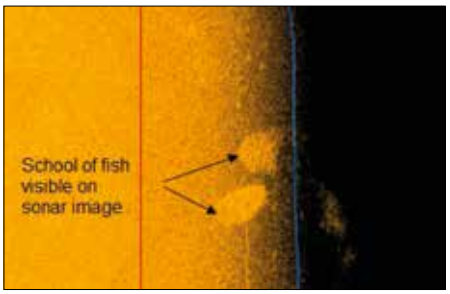

Fig. 15. School of fish visible on sonar image but not giving an acoustic shadow.

Usually, objects present stronger echoes than the bottom structure. However, an inverted presentation cannot be excluded. Some objects reflect less energy than the bottom around them. Fig. 16 presents a rubber wheel lying on a sandy bottom, an element that reflects less energy than more common objects on the sea floor.

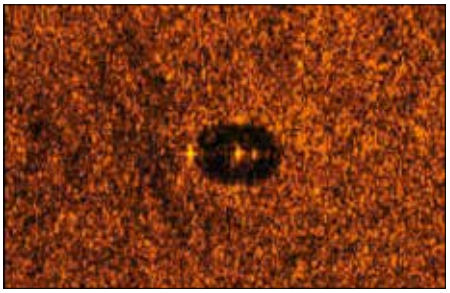

Fig. 16. Visualisation of rubber wheel, an element which produces weaker echo strength than other common objects on the sea floor.

The effectiveness of an AUV mission focused on collecting and analysing sonar data may be degraded due to the object characteristics or environmental factors, e.g. bottom composition. In that case, it is highly recommended to plan additional tracks, to observe the structure from other directions. An ideal solution, giving a more objective situational assessment, is to carry out the identification process by diverse or remotely operated vehicles (ROV) after detecting an object of interest. The experience gained during the aforementioned process helps the operators to increase their knowledge and efficiency of data analysis.

The visualisations of example objects are presented below (Fig. 17-18).

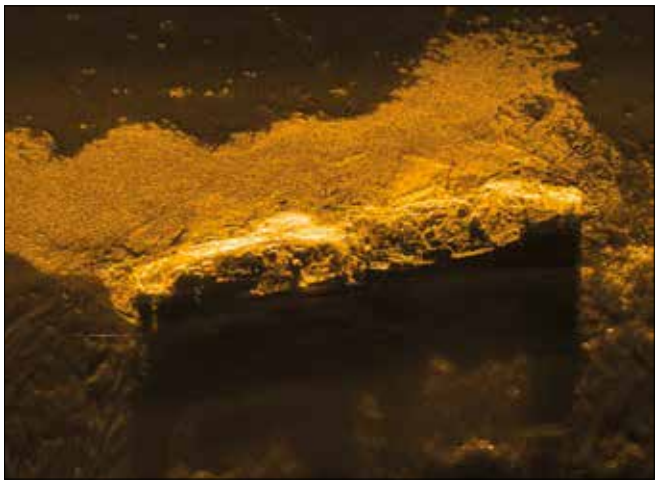

Fig. 17. Shipwreck surrounded by heavy fuel.

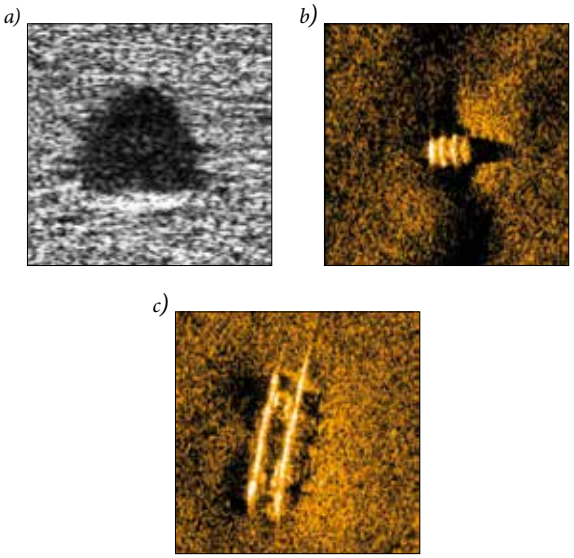

Fig. 18. Objects presented on sonar record: a) sea mine Manta type [21] b) barrel c) ladder.

PRESENTATION OF SEA FLOOR STRUCTURES ON SONAR IMAGES

Carrying out the interpretation process for sea floor structures, sonar users need to know about the process of visualisation of seabed projections and depressions. It may be the case that the acoustic shadow (or 'black hole') is visible on the screen but there is no possibility of finding the object which generated this shadow. In that case, it is highly probable that the operator recognises the depression of the seabed. In that case, the energy generated from the transmitter is dispersed inside the depression and does not give a visible shadow. Examples of this situation usually appear when the seabed structure is folded or in areas with wells and boreholes (Fig. 19).

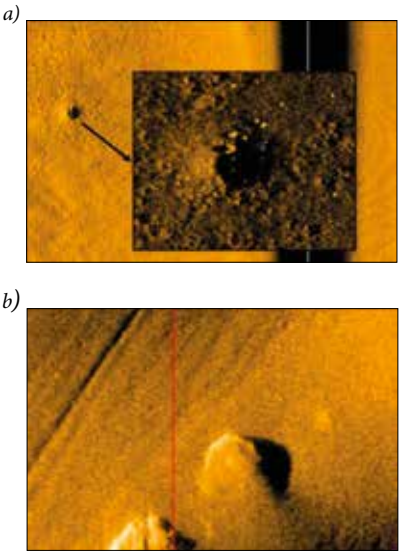

Fig. 19. a) Seabed depression visible on sonar record b) Seabed projection visible on sonar record.

A depression is usually presented on the sonar record with a strong echo on the outer part of the image, looking from the sonar side. The operator needs to consider how that image was generated, taking into account sonar beam characteristics, AUV movements and the basic principles associated with post-processed data. An acoustic shadow always appears behind the object; the opposite situation represents seabed depressions.

SUMMARY

It can be concluded that sonar imaging and processing is now an intensively explored topic. The use of autonomous vehicles for harbour and seaway traffic line monitoring is one of the most effective solutions, in terms of maintaining security awareness. This paper has contributed to the subject by presenting the concept of image reconstruction from data collected during AUV missions. For this purpose, a side-scan sonar, widely used to collect signals in aquatic environments, was used. With appropriate processing (including de-noising), collected data can be interpreted by inexperienced operators. However, it is highly recommended that users of sonar technology familiarise themselves with the methods and techniques that make that process more effective.

Although new techniques and programs provide dedicated solutions which help the process of data interpretation, the decisions regarding proper object classification still depend on the human factor. In order to ensure the correct assessment

and classification of objects on sonar imagery, the table below can be used.

Tab. 2. Sonar Contact Confidence Level Form

Sonar Contact Confidence Level					
Object no.	Shape	Shadow	Size	Echo Strength	Environment around object
Object 1					

New algorithms and programs, such as Automated Target Recognition (ATR) solutions, are still only advisory and the most appropriate mission analysis is based on the knowledge and experience of the operators [30, 31]. The paper presented includes guidelines and recommendations, which should be helpful for operators working with sonar data.

REFERENCES

1. P. Smith Menandro and A. Cardoso Bastos, "Seabed Mapping: A Brief History from Meaningful Words", *Geosciences*, vol. 10, no. 7, Art. no. 7, Jul. 2020, doi: 10.3390/geosciences10070273.

2. T. Kogut and K. Bakuła, "Improvement of Full Waveform Airborne Laser Bathymetry Data Processing based on Waves of Neighbourhood Points", *Remote Sens.*, vol. 11, no. 10, Art. no. 10, Jan. 2019, doi: 10.3390/rs11101255.

3. M. Żokowski, M. Chodnicki, P. Krogulec, and N. Sigiel, "Procedures concerning preparations of autonomous underwater systems to operation focused on detection, classification and identification of mine like objects and ammunition", J. *KONBiN*, vol. 48, pp. 149–168, Dec. 2018, doi: 10.2478/jok-2018-0051.

4. S. Sivčev, J. Coleman, E. Omerdić, G. Dooly, and D. Toal, "Underwater manipulators: A review", *Ocean, Eng.*, vol. 163, pp. 431–450, Sep. 2018, doi: 10.1016/j.oceaneng.2018.06.018.

5. C. Roman and R. Mather, "Autonomous Underwater Vehicles as Tools for Deep-Submergence Archaeology", *Proc. Inst. Mech. Eng. Part M J. Eng. Marit. Environ.*, vol. 224, no. 4, pp. 327–340, Nov. 2010, doi: 10.1243/14750902JEME202.

6. L. A. Gonzalez, "Design, Modelling and Control of an Autonomous Underwater Vehicle", Bachelor of Engineering Honours Thesis 2004, The University of Western Australia, 2004.

7. Y. Ji, S. Kwak, A. Yamashita, and H. Asama, "Acoustic camera-based 3D measurement of underwater objects through automated extraction and association of feature points", *IEEE Int. Conf. Multisens. Fusion Integr. Intell. Syst.*, vol. 0, pp. 224–230, 2016, doi: 10.1109/MFI.2016.7849493.

8. W. Kazimierski and G. Zaniewicz, "Determination of Process Noise for Underwater Target Tracking with Forward Looking Sonar", *Remote Sens.*, vol. 13, no. 5, Art. no. 5, Jan. 2021, doi: 10.3390/rs13051014.

9. T. Zhang, S. Liu, X. He, H. Huang, and K. Hao, "Underwater Target Tracking Using Forward-Looking Sonar for Autonomous Underwater Vehicles", *Sensors*, vol. 20, no. 1, p. 102, Dec. 2019, doi: 10.3390/s20010102.

10. O. Y. Sergiyenko and V. V. Tyrsa, "3D Optical Machine Vision Sensors with Intelligent Data Management for Robotic Swarm Navigation Improvement", *IEEE Sens. J.*, vol. 21, no. 10, Art. no. 10, 2021, doi: 10.1109/JSEN.2020.3007856.

11. K. Bikonis, M. Moszyński, and Z. Łubniewski, "Application of Shape From Shading Technique for Side Scan Sonar Images", *Pol. Marit. Res.*, vol. 20, pp. 39–44, 2013, doi: 10.2478/pomr-2013-0033.

12. G. Grelowska, E. Kozaczka, and W. Szymczak, "Acoustic Imaging of Selected Areas of Gdansk Bay with the Aid of Parametric Echosounder and Side-Scan Sonar", *Pol. Marit. Res.*, vol. 24, no. 4, pp. 35–41, Dec. 2017, doi: 10.1515/pomr-2017-0133.

13. J. M. Topple and J. A. Fawcett, "MiNet: Efficient Deep Learning Automatic Target Recognition for Small Autonomous Vehicles", *IEEE Geosci. Remote Sens. Lett.*, vol. 18, no. 6, pp. 1014–1018, Jun. 2021, doi: 10.1109/LGRS.2020.2993652.

14. H. Yu, Z. Li, D. Li, and T. Shen, "Bottom Detection Method of Side-Scan Sonar Image for AUV Missions", *Complexity*, vol. 2020, pp. 1–9, Oct. 2020, doi: 10.1155/2020/8890410.

15. X. Zhang, C. Tan, and W. Ying, "An Imaging Algorithm for Multireceiver Synthetic Aperture Sonar", *Remote Sens.*, vol. 11, no. 6, Art. no. 6, Jan. 2019, doi: 10.3390/rs11060672.

16. W. Chen, L. Wang, Y. Zhang, X. Li, J. Liu, and W. Wang, "Anti-disturbance grabbing of underwater robot based on retinex image enhancement", *Chinese Automation Congress (CAC)*, Nov. 2019, pp. 2157–2162. doi: 10.1109/CAC48633.2019.8997332.

17. X. Wang, Q. Li, J. Yin, X. Han, and W. Hao, "An Adaptive De-noising and Detection Approach for Underwater Sonar Image", *Remote Sens.*, vol. 11, no. 4, Art. no. 4, Jan. 2019, doi: 10.3390/rs11040396.

18. J. C. Isaacs, "Sonar automatic target recognition for underwater UXO remediation," in *2015 IEEE Conference on Computer Vision and Pattern Recognition Workshops (CVPRW)*, Jun. 2015, pp. 134–140. doi: 10.1109/CVPRW.2015.7301307.

19. A. Waite, *Sonar for Practising Engineers*, 3 rd. Wiley: Hoboken, NJ, USA, 2002. Accessed: Jun. 15, 2021. [Online].Available: https://www.wiley.com/en-us/ Sonar+for+Practising+Engineers%2C +3rd+Edition-p-9780471497509

20. R. Heremans, Y. Dupont, and M. Acheroy, "Motion Compensation in High Resolution Synthetic Aperture Sonar (SAS) Images". IntechOpen, 2009. doi: 10.5772/39408.

21. F. Florin, F. Fohanno, I. Quidu, and J. Malkasse, "Synthetic Aperture and 3D Imaging for Mine Hunting Sonar", *Engineering*, 2004, Accessed: Jun. 11, 2021. [Online]. Available: /paper/Synthetic-Aperture-and-3D-Imaging-for-Mine-Hunting-Florin-Fohanno/0cff43ea7dc424e21b9ed83d256a2e25eda4a312

22. M. Zieja, M. Ważny, and S. Stępień, "Outline of a method for estimating the durability of components or device assemblies while maintaining the required reliability level", *Eksploat. Niezawodn. - Maint. Reliab.*, vol. 20, no. 2, 2018, doi: 10.17531/ein.2018.2.11.

23. D. T. Cobra, A. V. Oppenheim, and J. S. Jaffe, "Geometric distortions in Side-Scan Sonar images: A Procedure for their estimation and correction", *J. Ocean. Eng.*, vol. 17, no. 3, 1992.

24. M. Machado, P. Drews-Jr, P. Núñez, and S. Botelho, "Semantic Mapping on Underwater Environment Using Sonar Data". 2016. doi: 10.1109/LARS-SBR.2016.48.

25. P. Blondel, *The Handbook of Sidescan Sonar.* Berlin Heidelberg: Springer-Verlag, 2009. doi: 10.1007/978-3-540-49886-5.

26. K. H. Talib, M. Y. Othman, S. A. H. Sulaiman, M. A. M. Wazir, and A. Azizan, "Determination of speed of sound using empirical equations and SVP", in *2011 IEEE 7th International Colloquium on Signal Processing and its Applications*, 2011, pp. 252–256.

27. R. J. Urick, *Principles of Underwater Sound*, 3rd ed. Peninsula Pub, 1996. Accessed: Jun. 03, 2021. [Online]. Available: https://www.abebooks.com/9780932146625/Principles-Underwater-Sound-3rd-Edition-0932146627/plp

28. X. Shang, J. Zhao, and H. Zhang, "Automatic Overlapping Area Determination and Segmentation for Multiple Side Scan Sonar Images Mosaic", *IEEE J. Sel. Top. Appl. Earth Obs. Remote Sens.*, vol. 14, pp. 2886–2900, 2021, doi: 10.1109/JSTARS.2021.3061747.

29. J. Tęgowski and A. Zielinski, "Synthesis And Wavelet Analysis Of Side-Scan Sonar Sea Bottom Imagery", *Hydroacoustics*, vol. 9, 2006.

30. A. K. Mishra and B. Mulgrew, "Automatic target recognition" in *Encyclopedia of Aerospace Engineering*, R. Blockley and W. Shyy, Eds. Chichester, UK: John Wiley & Sons, Ltd, 2010, p. eae281. doi: 10.1002/9780470686652.eae281.

31. T. Praczyk, "Correction of Navigational Information Supplied to Biomimetic Autonomous Underwater Vehicle", *Pol. Marit. Res.*, vol. 25, no. 1, pp. 13–23, Mar. 2018, doi: 10.2478/pomr-2018-0002.

CONTACT WITH THE AUTHORS

Mariusz Zieja
e-mail: mariusz.zieja@itwl.pl

Air Force of Technology
Warsaw
Poland

Wojciech Wawrzyński

Warsaw University of Technology
Warsaw
Poland

Justyna Tomaszewska

Military University of Aviation
Dęblin
Poland

Norbert Sigiel

MCM Squadron
Gdansk
Poland